Molecular Genetics and Metabolism Reports 27 (2021) 100742

Contents lists available at ScienceDirect

Molecular Genetics and Metabolism Reports

journal homepage: www.elsevier.com/locate/ymgmr

Clinical utility of brain MRS imaging of patients with adult-onset non-cirrhotic hyperammonemia

Andrew B. Stergachis [a,b,*], Joel B. Krier [c], Sai K. Merugumala [d], Gerard T. Berry [e], Alexander P. Lin [d,**]

[a] Division of Medical Genetics, Department of Medicine, University of Washington, Seattle, WA, USA
[b] Brotman Baty Institute for Precision Medicine, Seattle, WA, USA
[c] Division of Genetics, Department of Medicine, Brigham and Women's Hospital, Boston, MA, USA
[d] Department of Radiology, Brigham and Women's Hospital, Harvard Medical School, Boston, MA, USA
[e] Division of Genetics and Genomics, The Manton Center for Orphan Disease Research, Boston Children's Hospital, Harvard Medical School, Boston, MA, USA

ARTICLE INFO

Keywords:
Non-cirrhotic hyperammonemia
Urea cycle disorder
Magnetic resonance spectroscopy
Cerebral myo-inositol
Cerebral glutamine

ABSTRACT

Adult-onset non-cirrhotic hyperammonemia (NCH) is a rare, but often fatal condition that can result in both reversible and irreversible neurological defects. Here we present five cases of adult-onset non-cirrhotic hyperammonemia wherein brain magnetic resonance spectroscopy (MRS) scans for cerebral glutamine (Gln) and myo-inositol (mI) levels helped guide clinical management. Specifically, we demonstrate that when combined with traditional brain magnetic resonance imaging (MRI) scans, cerebral Gln and mI MRS can help disentangle the reversible from irreversible neurological defects associated with hyperammonemic crisis. Specifically, we demonstrate that whereas an elevated brain MRS Gln level is associated with reversible neurological defects, markedly low mI levels are associated with a risk for irreversible neurological defects such as central pontine myelinolysis. Overall, our findings indicate the utility of brain MRS in guiding clinical care and prognosis in patients with adult-onset non-cirrhotic hyperammonemia.

1. Introduction

Adult-onset non-cirrhotic hyperammonemia (NCH) is a rare, but often fatal condition that can arise in a variety of clinical settings including: adult-onset urea cycle defects [21]; urease-producing organism infections [12]; side effects of certain medications [6]; and severe nutritional deficiencies [20]. Patients with adult-onset non-cirrhotic hyperammonemia frequently present with hyperammonemic coma, and can develop irreversible neurological insults from cerebral edema, brain herniation and osmotic demyelination of the pons. Overall, prognosis is quite poor, with a mortality rate of 80% in a post-bone marrow transplant cohort [7], 50% in a post-Roux-en-Y gastric bypass (RYGB) cohort [9], and 39% in a combined adult-onset NCH cohort [20].

Distinguishing reversible from irreversible neurological defects in these patients is essential for appropriately guiding management decisions, and imaging strategies such as magnetic resonance spectroscopy (MRS) have been demonstrated to aid in this process. MRS is a method that uses conventional magnetic resonance imaging (MRI) scanners to measure the cerebral concentrations of highly abundant biological compounds. Cerebral glutamine (Gln) peaks are typically low under normal physiological states, but become prominent during acute hyperammonemic episodes due to the conversion of ammonia into glutamine by the enzyme glutamine synthetase [4,11]. In addition, chronic hyperammonemia has been associated with low cerebral myo-inositol (mI) levels on brain MRS imaging [2,10,11]. In prior reports, we and others have demonstrated cerebral Gln MRS as a noninvasive technique for monitoring cerebral Gln levels in association with hyperammonemia-induced altered mental status [10,14]. Despite the potential clinical utility of brain MRS in adult patients with non-cirrhotic hyperammonemia, there is currently a paucity of available data outside of patients with ornithine transcarbamylase (OTC)

Abbreviations: NCH, Non-cirrhotic hyperammonemia; Gln, Glutamine; mI, Myo-inositol; NAAG, N-acetylaspartylglutamate; NAA, N-acetylaspartate; PCG, Posterior cingulate gyrus; PWM, Parietal white matter; BG, Basal ganglia.

* Corresponding author at: Division of Medical Genetics, Department of Medicine, University of Washington, Seattle, WA, USA.
** Corresponding author.
E-mail addresses: absterga@u.washington.edu (A.B. Stergachis), aplin@bwh.harvard.edu (A.P. Lin).

https://doi.org/10.1016/j.ymgmr.2021.100742
Received 25 November 2020; Received in revised form 2 March 2021; Accepted 4 March 2021

deficiency [4,10]. To provide further clinical data on cerebral MRS imaging in adult patients with non-cirrhotic hyperammonemia, we present brain MRS results from 5 cases wherein this imaging has played a vital role in guiding clinical care decisions.

2. Patients and methods

2.1. Patients

Retrospective chart review and analysis of MRS imaging data was performed after institutional review board (IRB) approval. Cases were identified based on referral to the Genetics/Metabolism service for hyperammonemia management. Additional clinical, genetic, and biochemical information on these patients is published elsewhere [20], wherein patients 1, 2, 3, 4, and 5 in this cohort correspond to patients 15, 2, 7, 4, and 21 of the Stergachis et al. cohort, respectively. P-value for Fig. 4a was calculated using the corr.test function in R. All patients provided written informed consent for retrospective data evaluation.

2.2. MRS acquisition and processing

MRPAGE was acquired and reconstructed for localization of the MRS voxels. The volumes of interests were specified as 2x2x2 cc regions in the posterior cingulate gyrus, parietal white matter, and basal ganglia as shown in Fig. 1. These regions were selected based on previous literature that demonstrated their sensitivity to increased glutamine in the brain [10,18]. Single voxel point-resolved spectroscopy (PRESS) was acquired on 3T MRI scanner (Siemens Verio) using an echo time of 30 ms, repetition time of 2 s, 128 averages 2048 data points, and 1200 Hz spectral width. An unsuppressed water reference with 16 averages was acquired for quantitation. The RF coil consisted of a 32 channel ^{1}H tuned phased array head coil. B_0 shimming was performed with the DESS method. An

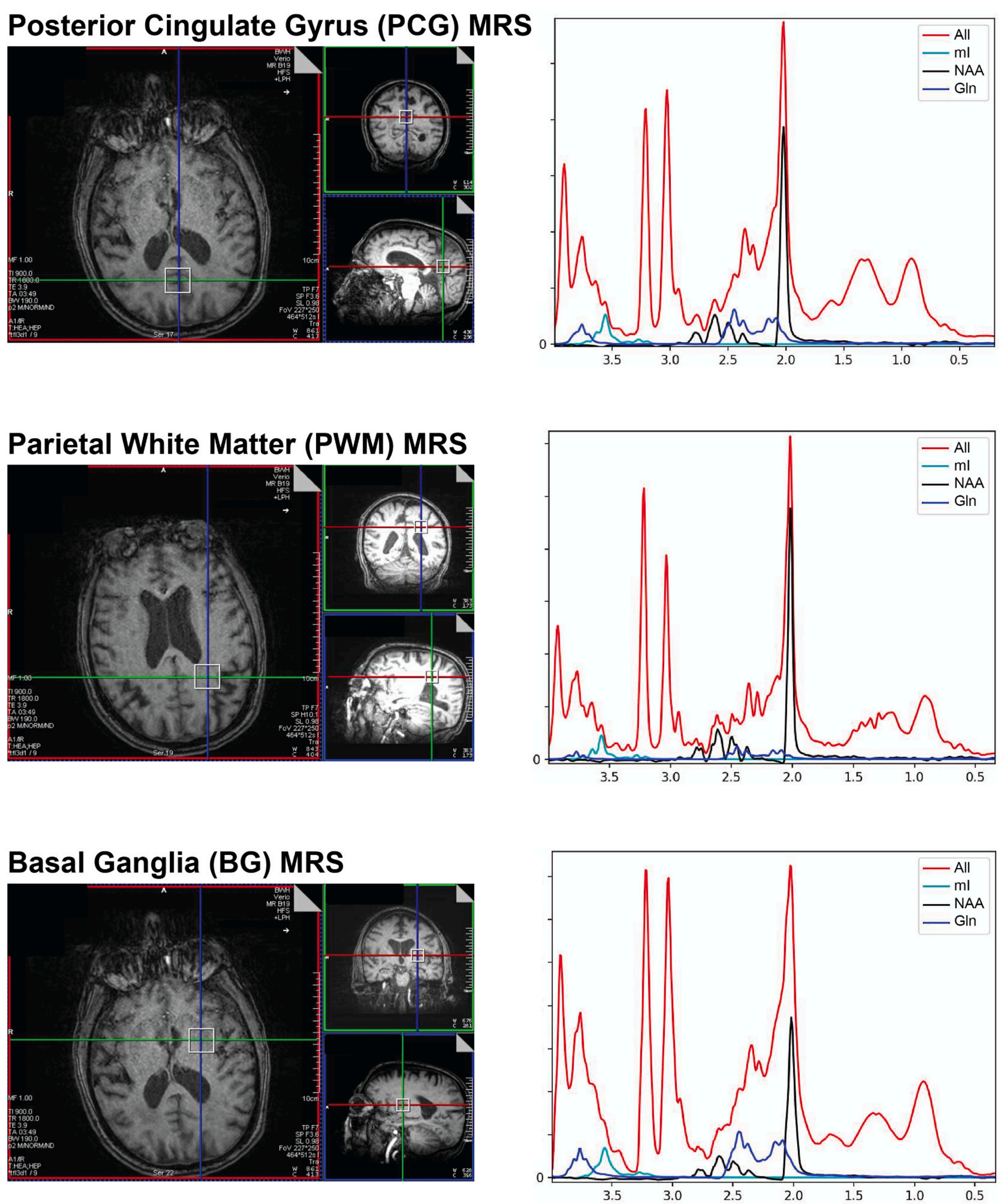

Fig. 1. Representative spectra from patient 1 from the three regions of interest measured in each patient. Left: Voxel location shown on T1 MPRAGE images. Right: MR spectra with metabolite fit for myo-inositol (mI), N-acetylaspartate (NAA), and glutamine (Gln).

initial automatic shim as attempted and manual shimming was performed when the automatic shim showed to be inadequate. WET, a B_1 independent water-suppression method was used [15].

Post processing was performed with Suspect software package (using Python and numpy). The raw, uncombined data acquired was used for this post processing pipeline. Processing steps included channel combination, frequency correction, averaging samples, residual water signal removal, and phase correction prior to metabolite fitting and quantification. Frequency correction was done during post processing by aligning the creatine metabolite resonance that was fitted with the HSVD method [19]. Metabolite concentrations of glutamine (Gln) as well as N-acetylaspartate (NAA), glutamate (Glu), creatine (Cr), choline (Cho), myo-inositol (mI), and other metabolites were estimated using the LCModel software package which performs linear combination analysis with a priori metabolite spectra [17]. The metabolite values are normalized to the unsuppressed water signal to determine absolute metabolite concentrations. This absolute concentration estimation was further adjusted with respect to the gray matter, white matter, and CSF partial-volume fractions (PVF) of the target voxel. Segmentation on the PVFs was performed on the 3D MPRAGE image, which was available for most cases (see Table 1), using the FSL software package to obtain these fractions and the following equation was used to calculate the partial-volume corrected absolute concentration:

$$C_c = C_{LCM}\left(\frac{55556\ \text{mM}}{35880\ \text{mM}}\right)\left[\ (1\cdot p_{CSF}) + (0.779\cdot p_{GM}) + (0.645\cdot p_{WM})\ \right]$$

where C_c is the corrected concentration, C_{LCM} is the LCModel estimated concentration, and p_{GM}, p_{WM}, and p_{CSF} correspond to the partial volumes of gray matter, white matter, and CSF, respectively. The 35,880 mM value corresponds to LCModel's assumed water concentration which is corrected to the actual value in CSF of 55,556 mM, approximately 77.9% of this in gray matter, and approximately 64.5% in white matter [8]. A phantom solution of 5 mM of glutamine and 10 mM of creatine was also scanned using the same sequences in order to validate the quantitation measures. Finally, a cohort of 22 healthy volunteers (ages 48–70 years) were also imaged using the same voxel locations and protocol to provide a normative range of values.

The quality of the data and metabolite fitting was performed by assessing using LCModel's reported Cramér–Rao lower bound (CRLB) value in addition to signal to noise ratio (SNR) and linewidth or full-width half max (FWHM) for each acquisition. All scans had NAA CRLB of less than 5%, SNR greater than 25, and FWHM of less than 0.05 Hz. Glutamine CRLB was 14.3% + 7.7% demonstrating that it was consistently fit and distinguishable from glutamate due its high concentration in most cases.

3. Results

3.1. Case 1

Patient 1 is a 44-year-old non-cirrhotic male with a history of dextro-transposition of the great arteries, status-post Mustard repair in infancy, who developed acute-onset altered mental status and status epilepticus three days post-orthotopic heart transplantation, and was found to have a plasma NH_3 level of >1320 μmoles/L. Tracheal secretions were positive for *U. urealyticum*, and he was managed with antibiotics, renal replacement therapy, ammonia scavengers, and hypothermic cooling, with gradual improvement and subsequent normalization of his NH_3 level after eight days of treatment [13]. Two days after hyperammonemia resolution he began following commands and slowly started to regain neurological function over the following several weeks. Brain MRS performed five days after resolution of his hyperammonemia demonstrated a mildly elevated posterior cingulate gyrus (PCG) Gln level of 4.76 mmoles/kg and a low PCG mI level of 1.22 μmoles/L (Fig. 1). Brain MRS performed seven days later demonstrated a normal PCG Gln level of 3.070 mmoles/kg and a persistently low PCG mI level of 1.209 mmoles/kg. Brain MRI demonstrated findings concerning for global hypoxia. After several months of recovery, he regained most of his prior neurological status, but had a new persistent frontal disinhibition.

3.2. Case 2

Patient 2 is a 53-year-old non-cirrhotic female with a history of alcohol use disorder and obesity, 6 years status-post RYGB surgery, who presented with an ischemic left foot requiring femoral-popliteal bypass surgery. Two weeks into her admission she developed altered mental status and was found to have an NH_3 level of 181 μmoles/L. Over the subsequent five days she became obtunded, with NH_3 levels peaking at 453 μmoles/L (Fig. 2a). Despite management with hemodialysis/hemofiltration plus ammonia scavengers, her NH_3 levels remained persistently elevated at ~160 μmoles/L for the subsequent five days. Initial brain MRS demonstrated a markedly elevated posterior cingulate gyrus (PCG) Gln level of 18.60 mmoles/kg and a low PCG mI level of 1.17 mmoles/kg (plasma NH_3 154 μmoles/L and plasma Gln 724 μmoles/L at time of MRS) (Table 1). Repeat brain MRS after 4 days of persistently elevated NH_3 levels and no neurological improvement demonstrated interval improvement of PCG Gln to 13.864 mmoles/kg and a persistently low PCG mI of 1.464 mmoles/kg (plasma NH_3 136 μmoles/L and plasma Gln 391 μmoles/L at time of MRS). Her NH_3 level subsequently normalized, accompanied by improvement in her mental status, with repeat brain MRS seven days after NH_3 level normalization demonstrated interval normalization of PCG Gln to 1.63 mmoles/kg, but a persistently low PCG mI of 1.00 mmoles/kg. Two weeks later, her NH_3 level briefly spiked to 199 μmoles/L, and brain MRS two days after this spike demonstrated a normal PCG Gln level of 2.13 mmoles/kg and a low but improving PCG mI level of 1.83 mmoles/kg. MRI at this time demonstrated concern for osmotic demyelination in the pons. Over the following two months her neurological status progressively improved to baseline and she was discharged to her home after a prolonged inpatient rehab stay.

3.3. Case 3

Patient 3 is a 68-year-old non-cirrhotic male with a history of chronic myelomonocytic leukemia who presented with somnolence and hypoxia in the setting of acute blast crisis. He was started on hydroxyurea and underwent leukapheresis, but despite improvements in his leukocyte count he developed worsening oliguric renal failure, hypoxemia and somnolence and was intubated and started on hemofiltration, at which time his NH_3 level was fond to be elevated to 100 μmoles/L. His NH_3 levels normalized after 48 h of hemofiltration, but he remained intubated due to persistent somnolence, prompting a brain MRS five days after normalization of his NH_3 level. Brain MRS demonstrated normal brain glutamine and myo-inositol levels. His mental status improved over the following 24 h, enabling extubation, and a return to baseline mental status over the following week. He subsequently changed his code status to DNR/DNI and died from hypoxemic respiratory failure three weeks later.

3.4. Case 4

Patient 4 is a 54-year-old non-cirrhotic male with a history of alcohol use disorder who presented with altered mental status, leukocytosis and lactic acidosis and was found to have an NH_3 level of 322 μmoles/L (Fig. 2b). Hemodialysis, which was initiated for NH_3 clearance, resulted in improved NH_3 levels, but no appreciable neurological improvement, prompting a brain MRS. Brain MRS demonstrated an elevated PCG Gln level of 6.75 mmoles/kg and a very low PCG mI level of 0.69 mmoles/kg (plasma NH_3 74 μmoles/L and plasma Gln 493 μmoles/L at time of MRS). His NH_3 level normalized over the following six days, but his mental status remained poor, prompting a repeat brain MRS, which

Table 1
Brain MRS and plasma metabolite concentrations for all 5 patients in this case series, as well as reference ranges derived from healthy control. MRS scan regions include the posterior cingulate gyrus (PCG), parietal white matter (PWM), and basal banglia (BG). Metabolites include glutamine (Gln), myoinositol (mI), total N-acetyl aspartate (NAA + NAAG), total choline (Cho + PCho), and total creatine (Cr + PCr). Each metabolite shows the concentration in the first column and the Cramer-Rao lower bound (%SD) in the second column. Scans that underwent partial-volume fractions (PVF) correction are indicated in the final column.

Case	Age/Sex	Peak NH_3 (μmol/L)	Day of MRS scan relative to initial NH_3	Plasma NH_3 at time of MRS scan (μmol/L)	Plasma Gln at time of MRS scan (μmol/L)	MRS scan region	MRS Gln (mmol/kg)	MRS Gln % SD	MRS mI (mmol/kg)	MRS mI % SD	MRS NAA + NAAG (mmol/kg)	MRS NAA + NAAG % SD	MRS Cho + PCho (mmol/kg)	MRS Cho + PCho % SD	MRS Cr + PCr (mmol/kg)	MRS Cr + PCr % SD	MRS PVF correction
Patient 1	44/M	>1320	Day 12	40	368	PCG	4.760	13	1.218	15	6.134	3	2.218	3	6.222	2	Yes
						PWM	1.668	27	0.776	20	7.505	3	2.267	2	3.996	3	Yes
						BG	3.244	15	0.733	22	2.870	7	1.438	3	3.600	4	Yes
			Day 19	20	N/A	PCG	3.070	19	1.209	16	5.407	5	1.675	3	6.432	2	No
						PWM	1.796	25	0.909	17	6.476	3	2.130	2	4.084	3	No
						BG	2.221	25	0.000	999	2.520	11	2.071	4	5.240	4	No
Patient 2	53/F	453	Day 9	154	724	PCG	18.603	3	1.168	13	5.733	3	0.748	4	5.491	2	Yes
						PWM	14.377	3	0.807	15	4.867	3	0.662	4	3.000	3	Yes
						BG	14.798	3	1.402	12	4.776	5	1.028	4	5.616	3	Yes
			Day 12	136	391	PCG	13.864	4	1.464	10	6.447	3	1.103	3	6.261	2	No
						PWM	12.617	4	0.844	14	6.431	3	1.091	3	4.162	3	No
						BG	9.161	4	1.311	13	5.712	5	1.177	5	5.791	4	Yes
			Day 22	28	218	PCG	1.628	23	0.999	13	6.017	3	1.472	3	5.108	2	Yes
						PWM	0.872	36	0.711	15	5.287	3	1.907	2	3.506	3	Yes
						BG	2.239	19	0.706	21	3.937	6	1.545	3	4.400	3	Yes
			Day 38	15	233	PCG	2.133	19	1.828	7	5.281	4	1.192	3	5.571	2	Yes
						PWM	2.112	15	1.115	11	4.381	5	1.988	2	4.340	3	Yes
						BG	3.079	16	1.591	12	4.359	6	1.270	4	5.006	3	Yes
			Day 76	49	820	PCG	4.905	10	3.676	5	6.573	3	1.016	4	5.146	2	Yes
						PWM	2.866	11	3.310	4	5.665	3	1.290	2	3.882	2	Yes
Patient 3	68/M	100	Day 7	24	N/A	PCG	2.050	22	2.721	6	6.137	3	1.337	3	6.262	2	Yes
						PWM	1.725	21	2.083	7	3.876	6	0.900	4	3.015	4	Yes
						BG	2.416	18	1.538	10	4.029	6	1.236	3	4.634	3	Yes
Patient 4	54/M	322	Day 6	74	493	PCG	6.746	6	0.687	20	3.725	4	1.120	3	4.796	2	Yes
						PWM	9.536	4	0.896	13	4.972	4	0.823	4	3.818	3	Yes
						BG	6.577	6	0.882	18	2.873	7	1.273	4	5.287	3	Yes
			Day 12	50	N/A	PCG	3.181	13	0.928	15	4.578	4	1.498	3	6.055	2	Yes
						PWM	2.570	16	0.626	23	4.527	4	1.486	3	3.506	3	Yes
						BG	3.149	14	0.000	999	1.700	11	1.242	4	3.951	3	Yes
Patient 5	66/M	956	Day 5	36	381	PCG	4.634	13	1.264	16	5.689	4	1.318	3	4.047	3	No
						PWM	7.537	6	0.767	19	6.816	3	1.379	3	2.977	3	No
						BG	6.912	12	1.239	24	7.75	6	1.598	5	6.320	4	No

		MRS Gln	MRS mI	MRS NAA + NAAG	MRS Cho + PCho	MRS Cr + PCr
Control Reference Ranges	PCG	2.020–3.340	3.256–5.368	6.281–9.471	0.871–1.372	4.707–6.577
	PWM	0.642–2.263	2.736–5.316	6.572–11.080	1.234–2.088	3.648–5.908
	BG	1.619–3.587	2.978–5.014	5.039–7.734	1.059–1.802	4.126–5.937

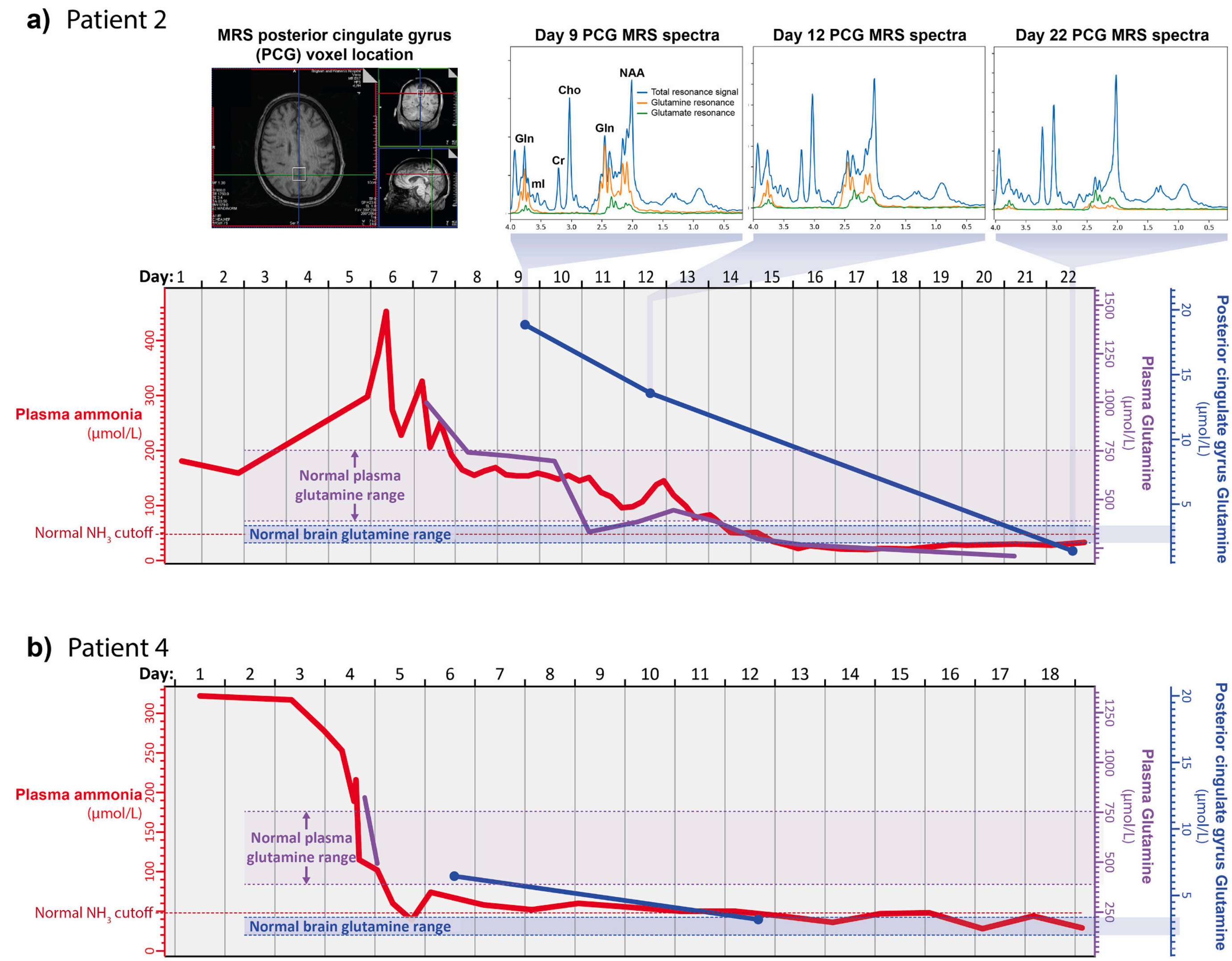

Fig. 2. Time course of plasma ammonia and glutamine levels as well as brain glutamine levels in (a) patient 2 and (b) patient 4. Plasma ammonia levels are in red, plasma glutamine levels in purple and brain glutamine levels from the PCG blue. Reference ranges for all three metabolites are indicated by dashed lines and shaded boxes. (For interpretation of the references to color in this figure legend, the reader is referred to the web version of this article.)

demonstrated mildly elevated parietal white matter (PWM) Gln level of 2.57 mmoles/kg and a persistently low PCG mI level of 0.93 mmoles/kg. Brain MRI demonstrated a new T2 abnormality at the central pons concerning for osmotic demyelination syndrome. Given poor neurological recovery, he underwent a tracheostomy and percutaneous gastrostomy placement and had a course complicated by multiple cardiac arrests, bacteremia and was eventually transitioned to comfort measures only.

3.5. Case 5

Patient 5 is a 66-year-old non-cirrhotic male without a significant past medical history who presented with two weeks of altered mental status and somnolence and was found to have an NH_3 level of 230 μmoles/L. He was started on ammonia scavenger therapy with initial improvement in ammonia levels to 20 μmoles/L, which quickly rebounded to 956 μmoles/L over the following 24 h, resulting in cerebral edema and seizures. Hemodialysis was then initiated, resulting in NH_3 level improvement to 68 μmoles/L. He was subsequently transferred to our institution, and on arrival he was obtunded with a normal NH_3 level. Brain MRS, performed 3 days after transfer demonstrated a mildly elevated PCG Gln level of 4.634 mmoles/kg and a low PCG mI level of 1.264 mmoles/kg (plasma NH_3 36 μmoles/L and plasma Gln 381 μmoles/L at time of MRS). Brain MRI demonstrated diffuse cerebral edema. He continued to show no neurological improvement and repeat brain MRI seven days later showed persistent cerebral edema. 14 days after transfer to our institution he continued to show no neurological improvement despite maintaining a normal NH_3 level, prompting transition to comfort measures only. Genetic testing demonstrated a hemizygous pathogenic *OTC* c.119G > A (p.R40H) variant, diagnostic of ornithine transcarbamylase (OTC) deficiency.

3.6. Comparison of brain glutamine and myo-inositol levels

Serial MRS scans were available for three of the cases, which enabled us to quantify the rate of recovery for cerebral Gln and mI levels after resolution of a hyperammonemic crisis. Notably, for patient 2, whereas cerebral Gln levels normalized by the third MRS scan (performed on day 22 of illness course), brain mI levels did not normalize until the fifth brain MRS scan, which was performed on day 76 of her illness course (Fig. 3a). Similarly, for patient 4 and 1, brain Gln levels normalized by day 12 and 19 respectively, yet brain mI levels remained persistently low in both of these patients on repeat imaging (Fig. 3b and c). In addition, Gln and mI levels were not significantly correlated with each

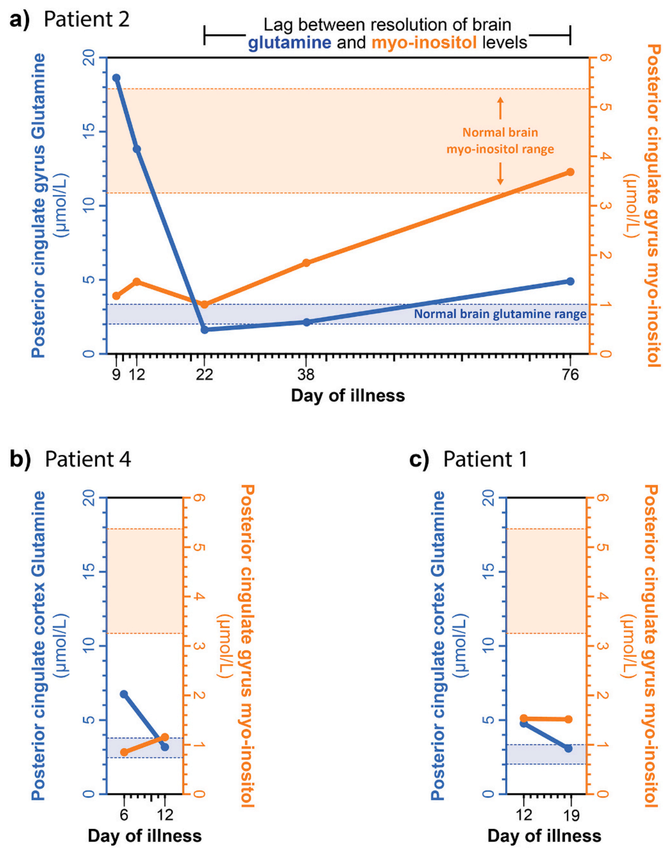

Fig. 3. Comparison of brain glutamine and myo-inositol levels between brain MRS scans in (a) patient 2, (b) patient 4, and (c) patient 1. Brain glutamine levels from the PCG are in blue, and brain myo-inositol levels from the PCG are in orange. Reference ranges for both metabolites are indicated by dashed lines and shaded boxes. (For interpretation of the references to color in this figure legend, the reader is referred to the web version of this article.)

other (Fig. 4a), indicating that cerebral mI levels in this cohort may be driven by more than the acute hyperammonemic event. Overall, these findings expose a lag time between the normalization of brain Gln and mI levels, during which time the brain may be at a particularly high risk for osmotic-mediated complications.

3.7. *Cerebral myo-inositol levels versus irreversible neurological outcomes*

To evaluate whether low cerebral mI levels could predispose to osmotic-related neurological complications, we visualized the relationship between initial brain MRS mI levels and long-term neurological complications for all five patients plus one previously published case [14]. Notably, whereas the two cases with the highest cerebral mI levels developed no long-term neurological complications, the cases with the lowest cerebral mI levels all developed neurological complications, with the two cases with the lowest mI levels developing osmotic demyelination (Fig. 4b).

4. Discussion

We present 5 cases of non-cirrhotic hyperammonemia wherein brain MRS imaging helped guide clinical management by disentangling the reversible from irreversible neurological defects associated with hyperammonemic crisis. Specifically, brain MRS Gln levels were especially useful in evaluating for reversible causes of neurological defects, and were more reliable than plasma ammonia or plasma glutamine levels for monitoring tissue stores of ammonia. For example, for patient 2, repeat brain MRS imaging during her acute hyperammonemic episode provided real-time evidence of successful total body ammonia clearance despite no significant changes in her blood ammonia level or mental status. Similarly, for patient 4, brain MRS imaging revealed significant residual glutamine stores, despite substantial improvement in blood ammonia levels, indicating further need for ammonia clearing therapies.

Brain MRS imaging was also useful in framing discussions regarding neurological prognosis with families. For example, for patient 1, normalization of brain Gln levels provided evidence to the clinical team of sustained recovery from his profound hyperammonemic episode. Similarly, for patient 3, normalized brain Gln levels indicated that his neurological status should quickly improve if it was mediated by hyperammonemia, which it did, enabling him to recover to a point where he was able to participate in his own goals of care conversations. In contrast, patients 4 and 5 both had largely normalized brain Gln levels, yet failed to show any significant neurological recovery over the following weeks, which was helpful in framing the relatively poor neurological prognosis to their families.

In addition, we observed that brain MRS mI levels may be useful in identifying patients at risk for irreversible neurological complications. Both mI and Gln are osmotic compounds that appear to compensate each

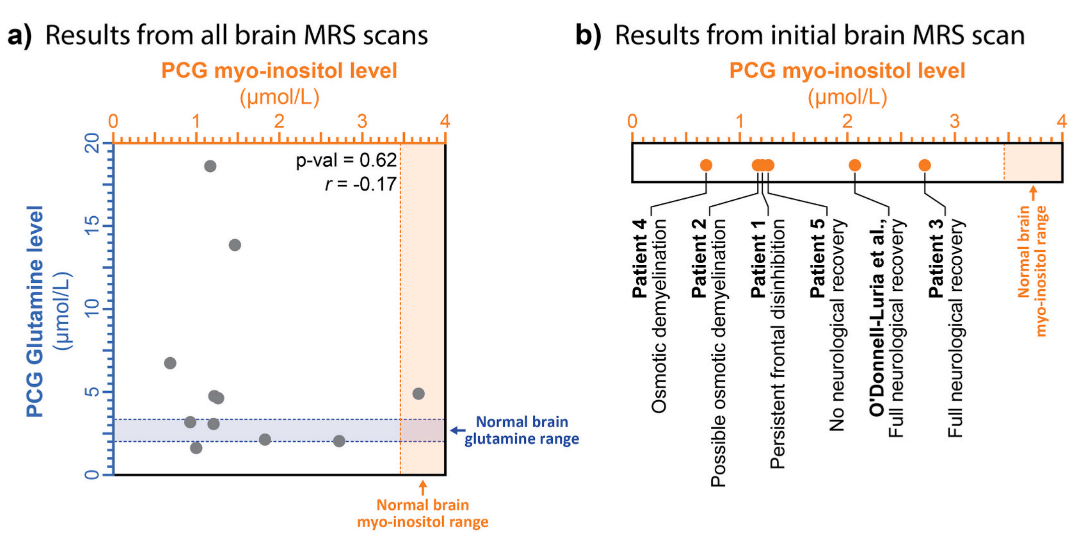

Fig. 4. Association between cerebral myo-inositol levels and irreversible neurological outcomes. (a) Scatterplot showing the relationship between brain MRS myo-inositol and glutamine levels. P-value and Pearson's correlation also displayed. (b) plot showing the initial brain MRS myo-inositol level within the PCG region, as well as any long-term neurological sequalae or MRI findings of demyelination.

other during hyperammonemic episodes [10,11], and studies in rats have previously shown that induced episodes of prolonged hyperammonemia result in elevated brain Gln levels and decreased brain mI levels [5]. However, we observed that whereas cerebral Gln levels can correct over a period of days to weeks, cerebral mI levels can take weeks to months to fully correct. This lag time between the normalization of brain Gln and mI levels may put brain tissue at a particularly high risk for osmotic-mediated complications, which is a known rare complication of hyperammonemic episodes [3]. Our findings suggest that very low brain MRS mI levels should be viewed as a potential risk factor for the subsequent development of osmotic demyelination upon resolution of a hyperammonemic crisis.

Several of the patients in this case series had two or more MRS scans performed, which were separated by 3 to 38 days apart. As discussed above, the data from these repeat scans were used to guide ongoing clinical care, and repeat scans were primarily initiated based on new neurological findings, and/or persistently poor neurological status or metabolic features. Notably, one of the major limitations to performing MRS imaging in this cohort was hemodynamic instability, which was frequently observed in this cohort, and limited their safe transportation to the MRI instrument.

Although brain MR spectroscopy is an emerging imaging modality in the evaluation of hyperammonemia, MRS imaging is currently utilized across multiple disciplines, including oncology, neurology, and pediatric genetics [1,16] for evaluating numerous metabolites including N-acetyl aspartate, choline, myo-inositol, creatinine, lactate, glutamate, and glutamine. Overall, our findings build upon this literature by indicating the additional utility of brain MR spectroscopy in guiding clinical care and prognosis in patients with adult-onset non-cirrhotic hyperammonemia.

Author's contributions

APL collected the data. APL, SKM, and ABS analyzed the data. ABS wrote the manuscript. ABS, GTB, and JBK contributed to the management of the patients. All authors read and approved the final manuscript.

Declaration of Competing Interest

All authors declare that they have no conflict of interest.

Acknowledgements

We thank the patients and their families. ABS is supported by NIH grants GM007748 and OD029630, and holds a Career Award for Medical Scientists from the Burroughs Wellcome Fund. GTB was supported by NIH NICHD grant 5U54HD061221-15.

References

[1] P.B. Barker, A. Bizzi, N. De Stefano, et al., Clinical MR Spectroscopy: Techniques and Applications, Cambridge University Press, 2009.

[2] O. Braissant, V. Rackayová, K. Pierzchala, et al., Longitudinal neurometabolic changes in the hippocampus of a rat model of chronic hepatic encephalopathy, J. Hepatol. 71 (2019) 505–515, https://doi.org/10.1016/j.jhep.2019.05.022.

[3] J.F. Cardenas, J.B. Bodensteiner, Osmotic demyelination syndrome as a consequence of treating hyperammonemia in a patient with ornithine transcarbamylase deficiency, J. Child Neurol. 24 (2009) 884–886, https://doi.org/10.1177/0883073808331349.

[4] A. Connelly, J.H. Cross, D.G. Gadian, et al., Magnetic resonance spectroscopy shows increased brain glutamine in ornithine carbamoyl transferase deficiency, Pediatr. Res. 33 (1993) 77–81, https://doi.org/10.1203/00006450-199301000-00016.

[5] J. Córdoba, J. Gottstein, A.T. Blei, Glutamine, *myo* -inositol, and organic brain osmolytes after portocaval anastomosis in the rat: implications for ammonia-induced brain edema, Hepatology 24 (1996) 919–923, https://doi.org/10.1002/hep.510240427.

[6] D.L. Coulter, R.J. Allen, Hyperammonemia with valproic acid therapy, J. Pediatr. 99 (1981) 317–319.

[7] S.M. Davies, E. Szabo, J.E. Wagner, et al., Idiopathic hyperammonemia: a frequently lethal complication of bone marrow transplantation, Bone Marrow Transplant. 17 (1996) 1119–1125.

[8] T. Ernst, R. Kreis, B.D. Ross, Absolute quantitation of water and metabolites in the human brain. I. Compartments and water, J. Magn. Reson. Ser. B 102 (1993) 1–8, https://doi.org/10.1006/JMRB.1993.1055.

[9] A.Z. Fenves, O.A. Shchelochkov, A. Mehta, Hyperammonemic syndrome after Roux-en-Y gastric bypass, Obesity 23 (2015) 746–749, https://doi.org/10.1002/oby.21037.

[10] A.L. Gropman, S.T. Fricke, R.R. Seltzer, et al., 1H MRS identifies symptomatic and asymptomatic subjects with partial ornithine transcarbamylase deficiency, Mol. Genet. Metab. 95 (2008) 21–30, https://doi.org/10.1016/J.YMGME.2008.06.003.

[11] R. Kreis, N. Farrow, B.D. Ross, Localized1H NMR spectroscopy in patients with chronic hepatic encephalopathy. Analysis of changes in cerebral glutamine, choline and inositols, NMR Biomed. 4 (1991) 109–116, https://doi.org/10.1002/nbm.1940040214.

[12] G.R. Lichtenstein, Y.X. Yang, F.A. Nunes, et al., Fatal hyperammonemia after orthotopic lung transplantation, Ann. Intern. Med. 132 (2000) 283–287.

[13] R.J. Madathil, L.G. Gilstrap, M.P. Pelletier, M.R. Mehra, Isolated hyperammonemic encephalopathy in heart transplantation, J. Hear Lung Transplant 37 (2018) 427–429, https://doi.org/10.1016/j.healun.2017.12.001.

[14] A.H. O'Donnell-Luria, A.P. Lin, S.K. Merugumala, et al., Brain MRS glutamine as a biomarker to guide therapy of hyperammonemic coma, Mol. Genet. Metab. 121 (2017) 9–15, https://doi.org/10.1016/j.ymgme.2017.03.003.

[15] R.J. Ogg, P.B. Kingsley, J.S. Taylor, WET, a T1- and B1-insensitive water-suppression method for in vivo localized 1H NMR spectroscopy, J. Magn. Reson. B 104 (1994) 1–10, https://doi.org/10.1006/jmrb.1994.1048.

[16] G. Oz, J.R. Alger, P.B. Barker, R. Bartha, A. Bizzi, C. Boesch, P.J. Bolan, K. M. Brindle, C. Cudalbu, A. Dinçer, U. Dydak, U.E. Emir, J. Frahm, R.G. González, S. Gruber, R. Gruetter, R.K. Gupta, A. Heerschap, A. Henning, H.P. Hetherington, F. A. Howe, P.S. Hüppi, R.E. Hurd, K. Kantarci, D.W. Klomp, R. Kreis, M. J. Kruiskamp, M.O. Leach, A.P. Lin, P.R. Luijten, M. Marjańska, A.A. Maudsley, D. J. Meyerhoff, C.E. Mountford, S.J. Nelson, M.N. Pamir, J.W. Pan, A.C. Peet, H. Poptani, S. Posse, P.J. Pouwels, E.M. Ratai, B.D. Ross, T.W. Scheenen, C. Schuster, I.C. Smith, B.J. Soher, I. Tkáč, D.B. Vigneron, R.A. Kauppinen, MRS Consensus Group, Clinical proton MR spectroscopy in central nervous system disorders, Radiology 270 (3) (2014) 658–679, https://doi.org/10.1148/radiol.13130531.

[17] S.W. Provencher, Automatic quantitation of localized in vivo 1H spectra with LCModel, NMR Biomed. 14 (2001) 260–264, https://doi.org/10.1002/nbm.698.

[18] B.D. Ross, S. Jacobson, F. Villamil, et al., Subclinical hepatic encephalopathy: proton MR spectroscopic abnormalities, Radiology 193 (1994) 457–463, https://doi.org/10.1148/radiology.193.2.7972763.

[19] B.C. Rowland, H. Liao, F. Adan, et al., Correcting for frequency drift in clinical brain MR spectroscopy, J. Neuroimaging 27 (2017) 23–28, https://doi.org/10.1111/jon.12388.

[20] A.B. Stergachis, K.M. Mogensen, C.C. Khoury, et al., A retrospective study of adult patients with noncirrhotic hyperammonemia, J. Inherit. Metab. Dis. 43 (2020) 1165–1172, https://doi.org/10.1002/jimd.12292.

[21] M.L. Summar, D. Dobbelaere, S. Brusilow, B. Lee, Diagnosis, symptoms, frequency and mortality of 260 patients with urea cycle disorders from a 21-year, multicentre study of acute hyperammonaemic episodes, Acta Paediatr. 97 (2008) 1420–1425, https://doi.org/10.1111/j.1651-2227.2008.00952.x.